PHYSICAL REVIEW A VOLUME 23, NUMBER 6 JUNE 1981

Differential cross sections for electron capture from helium by 25- to 100-keV incident protons

P. J. Martin, K. Arnett,* D. M. Blankenship, T. J. Kvale, J. L. Peacher, E. Redd, V. C. Sutcliffe,† and J. T. Park
Physics Department, University of Missouri-Rolla, Rolla, Missouri 65401

C. D. Lin and J. H. McGuire
Department of Physics, Kansas State University, Manhattan, Kansas 66506
(Received 13 January 1981)

Experimentally and theoretically determined differential cross sections are reported for electron capture in collisions of protons with helium atoms for incident proton energies of 25, 30, 50, and 100 keV and for center-of-mass scattering angles of 0.0 to 2.0 mrad. The magnitudes of the experimentally determined differential cross sections decrease from 10^{-10} to 10^{-12} cm^2/sr within the 0.0–0.8-mrad range of the center-of-mass scattering angle. At approximately 0.8 mrad a distinct change in the slope of the differential cross section is observed. The experimental results which are for capture into all bound states of hydrogen are compared with the theoretical results of a calculation for capture into the ground state using the two-state two-center atomic expansion method in the eikonal approximation. Good agreement between the theoretical and the experimental results is obtained with a static potential which accounts for screening of the helium nucleus by a single passive electron.

INTRODUCTION

The electron-capture process in collisions between protons and helium atoms in the incident velocity range $0.9 \leq v \leq 3.5$ a.u. (20–300 keV) has been the subject of many theoretical and experimental studies.[1-19] Results in this velocity range which are differential in scattering angle can be divided into two angular regions: (1) the large-scattering-angle domain and (2) the very small-scattering-angle domain. The large-scattering-angle domain is marked by violent collisions.[1-5] Because a one-to-one relationship between the scattering angle and the impact parameter is allowed for these collisions, semiclassical methods in which the nuclear motion is described classically may be applied to the study of the electron-capture process.[17] The small-scattering-angle domain is distinguished by angular distributions which are sharply peaked in the forward direction.[9,10] It should be noted that the value of the total cross section for the electron-capture process is determined in this region of the scattering angle. Because the impact parameter does not have a one-to-one relationship to the scattering angle in the small-scattering-angle domain, techniques which are analogous to the Van de Hulst extension of the Rayleigh-Gans[20] scattering of light (the eikonal approximation) are employed to relate impact-parameter calculations to experimentally determined differential cross sections.

The most basic test of the applicability of a theory for a scattering process is that the theoretically determined values of both the *total* cross section and the *differential* cross section compare favorably with the corresponding experimentally accepted result. A single experimentally determined differential cross section for electron capture by protons from helium atoms at very small-scattering angles has been reported by Bratton *et al.*[10] The 293-keV protons used in this work place this result at the high velocity (3.49 a.u.) end of the intermediate velocity range. The lack of experimentally determined differential cross sections at very small scattering angles over virtually all of the intermediate velocity range for collisions between protons and helium atoms has prompted the experimental work reported in this paper.

The present experiment involves a measurement of the angular distribution of fast hydrogen atoms formed in the collision

$$H^+ + He \rightarrow H(\theta) + He^+$$

for incident proton energies of 25, 30, 50, and 100 keV and center-of-mass scattering angles of 0–2 mrad. The differential ion energy-loss spectrometer located at the University of Missouri-Rolla[21] has been modified so that the angular distribution of the scattered fast atom products of ion-atom collisions can be measured. The design of the apparatus used to detect these scattered fast atoms allows measurements to be made in the forward direction including zero angle with an angular resolution of 120 μrad and an angular precision of 3.3 μrad. Techniques[21-24] previously developed for obtaining differential cross sections from scattered-ion angular distributions have been employed to obtain the experimentally determined differential cross sections presented in this paper.

Following the experimental work of Bratton *et al.*,[10] there have been several corresponding theoretical investigations of the differential cross section for electron capture. The early work of

Belkic and Salin[25] and Rogers and McGuire[13] demonstrated the effect of the internuclear potential on the calculated angular dependence of the differential cross section. In the later work of Belkic and Salin[14] and Belkic *et al.*,[18] the continuum-distorted-wave (CDW) method was used to calculate the total as well as differential cross sections. Lin, Soong, and Tunnell[15] and Lin and Soong,[16] using the two-state two-center atomic expansion (TSAE) method have also obtained the differential cross sections for this system at 293 keV. All of the above theories adopted the eikonal approximation in describing the scattering of the heavy particles, with the electron-capture amplitudes calculated in the impact-parameter formulation.

The CDW results of Belkic and Salin[14] and Belkic *et al.*,[18] and the TSAE results of Lin and Soong[16] were both in good agreement with the experimental results of Bratton *et al.*[10]; however, it must be pointed out that the CDW method is a perturbation calculation. Therefore, the CDW method is not expected to be valid at the lower end of the intermediate velocity range where the electron-capture probabilities are not small.[1-5] In fact, in collisions of protons with helium atoms, the total cross section for electron capture to the ground state obtained in the CDW approach differs significantly from the accepted experimental value for the total cross section for capture into all states.[18] The TSAE approach,[15,16] on the other hand, is expected to provide reasonable results at these lower velocities. The possibility of testing the TSAE method at lower velocities by comparing its results with the results of the present experiment has prompted the collaboration of the theoretical and experimental efforts reported in this paper.

EXPERIMENTAL METHOD

The experimental results reported in this paper were obtained at the ion energy-loss spectrometer laboratory in the Department of Physics at the University of Missouri-Rolla (UMR). Only the additions to this apparatus which were necessary for the present experiment and the improvements to the method of data acquisition employed in this laboratory are briefly discussed in the following section of this paper.

Figure 1 is a schematic of the ion energy-loss spectrometer in the latest configuration. The present additions to the apparatus include the neutral-particle detector with its associated beam defining slits and electronics and an incident ion-beam current monitor.

The scattered fast atoms resulting from electron-capture processes are separated from the scattered ions by the analyzing magnet. An assembly of movable-crossed slits is used to define the scattering solid angle of the neutral detector. The present slit dimensions are 5.08 $\times 10^{-3}$ cm in both the vertical and horizontal directions. This slit assembly is located 168 cm from the scattering center. The effect of this apparatus geometry on the scattered fast neutral beam is taken into account by a method which has been reported previously in Refs. 21–24.

The neutral particles are detected with an 18 stage venetian blind electron multiplier.[26] Owing to the intensity of the scattered neutral flux, a

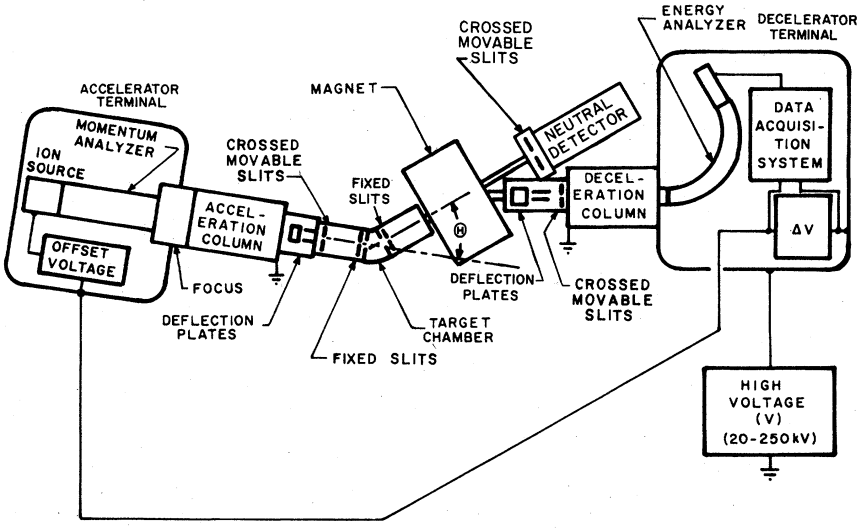

FIG. 1. Schematic drawing of the UMR variable angle ion energy-loss spectrometer.

current measuring configuration of the electron multiplier is required. The multiplier current is integrated and digitized by a fast picoammeter, a voltage to frequency converter, and a frequency counter. This digital information is accumulated and stored by the data acquisition program which is run on a controlling minicomputer.

The target chamber employed in the present experiment has been discussed in Ref. 23. While this chamber was designed for the production of an atomic hydrogen target, its use provides no complications for the reported experiment.

An analysis of previously reported differential cross sections[23,24] using the UMR ion energy-loss spectrometer has indicated that a source of measurement error is related to the monitoring of the incident beam. Using a recently installed incident beam-current monitor, this source of error has been virtually eliminated. The monitor is a biased Faraday cup which can be positioned under computer control to intercept the incident ion beam at the entrance to the scattering chamber. The Faraday cup is located behind the entrance collimating slit and hence intercepts the actual incident beam. The beam-monitor current is measured by an electrometer which is connected to the current digitizing electronics used for the neutral measurement. Because the ion current at the entrance of the scattering chamber is independent of the scattering angle, monitoring this current provides the information necessary to account for variations in the incident beam current over the course of the measurement.

With the present additions to the apparatus a new data acquisition program for the controlling minicomputer was required. For each value of the scattering angle, measurements are made both with and without target gas at the kinematic energy loss and at the excitation energy loss (see Refs. 21 and 24). Program control of both the number and duration (gate time) of these measurements of the detected signals permits the duty cycle of the apparatus to be optimized. The new data acquisition program allows the measurement of the statistical distribution of the detected ion signal and the detected neutral signal at each scattering angle. Values of the measured distribution which are greater than that allowed by Chauvenet's criterion[27] are discarded without replacement and the mean value and deviation of the corrected distribution are calculated and subsequently recorded. This process is repeated for each value of the scattering angle.

The present improvements in the data acquisition program combined with the incident beam monitor have resulted in both an increase in the usable angular range of the apparatus and a decrease in the standard deviation of the mean for the reported experimentally determined differential cross sections.

DATA ANALYSIS

The data resulting from the measurement of the angular distribution of the scattered fast neutral atoms are analyzed precisely in the same manner as reported in Ref. 21. It has been demonstrated in Ref. 24 that the limit of the validity of this method of data analysis is approached when the measured half-width of the scattered angular distribution equals that of the incident beam. This limit has not been exceeded in the present experiment.

In the data analysis method[21] a distinction is made between the "apparent" differential cross section and the "true" differential cross section. For the present work the apparent differential cross section is defined as

$$\frac{dS_n(\theta)}{d\Omega}=\frac{I_n(\theta)}{nl\Delta\Omega_n I},$$

where $I_n(\theta)$ is the measured neutral detector current, I is the integrated transmitted incident beam current, n is the target gas density, l is the length of the collision region, and $\Delta\Omega_n$ is the neutral detector solid angle.

The data analysis method employed[21] relates this apparent result to the true angular differential cross section for the process, $d\sigma/d\Omega$. The analytical representation of $dS/d\Omega$ involves an integration of the true angular differential cross section over the angular distribution of the incident beam and the solid angle subtended by the detector window. A numerical method has been developed to extract $d\sigma/d\Omega$ by equating the measured $dS/d\Omega$ to its integral representation at each acquisition angle with an assumed form for $d\sigma/d\Omega$.[21]

For the present experiment the detector efficiencies are not known to any degree of accuracy. Therefore, the final value of the true differential cross section is obtained by normalizing the integral of the present relative values to the experimentally accepted values of the total cross section for capture into all bound states reported in Ref. 8.

The angular distribution is measured at both positive and negative scattering angles, for any given run, hence it is possible to locate the exact 0° scattering angle with very high precision from the symmetry of the measured angular distribution. Owing to the very high angular resolution of the UMR differential ion energy-loss spectrometer, there are slight variations in the absolute measurement angle relative to the absolute 0° position be-

tween data sets. In order that the various data sets from different runs can be averaged together an interpolation of the measured data is used to adjust all measurements to the same set of laboratory angles. The reported measurements reflect the laboratory angles at which the actual data were taken. The adjusted values are averaged together and a standard deviation is calculated. These average values with standard deviation are the experimental values reported in the present work.

THEORY

Differential cross sections for heavy ion-atom collisions can be calculated directly in a quantum formulation of the scattering process; however, most of the current sophisticated theoretical models for charge-transfer processes are formulated in the impact-parameter (IP) approximation.[11-19] In the impact-parameter approximation the heavy particle motion is described by the classical equation of motion in an internuclear potential $W(R)$. This potential provides for the deflection of the projectile. However, for collisions at medium and high velocities rectilinear trajectories are used in the IP calculations and the deflection due to $W(R)$ is not considered. Therefore, in the pure IP formulation it is not possible to describe the angular distribution for the charge-transfer process. This difficulty is removed by resorting to the eikonal approximation, as formulated by Schiff,[28] Glauber,[29] and McGuire and Weaver.[30] These authors employed a partial-wave analysis in which the summation over partial waves is replaced by an integral and the Legendre polynomials by their asymptotic form to derive an expression for $d\sigma/d\Omega$. McCarroll and Salin,[31] Wilets and Wallace,[32] and Chen and Watson[33] also derived the desired equation from the full quantum formalism in which all quantities are replaced by their limits as the mass of the atomic nuclei becomes infinite. The resulting equation for differential cross sections for capture into the ground state in the center-of-mass (c.m.) system in atomic units is

$$\left(\frac{d\sigma}{d\Omega}\right)_{\text{c.m.}} = \left| i\mu v \int_0^\infty b\, db\, e^{2i\delta(b)} A(b) J_0\left(2\mu v b \sin\frac{\theta}{2}\right)\right|^2 \times (a_0^2\ \text{sr}^{-1}), \quad (1)$$

where μ is the reduced mass, b is the impact parameter, v is the relative velocity of the colliding nuclei, θ is the scattering angle, $A(b)$ is the scattering amplitude, and J_0 is the zeroth-order Bessel function. The eikonal phase is

$$\delta(b) = -\frac{1}{v}\int_b^\infty W(R)\,dz, \quad (2)$$

where $R = (b^2+z^2)^{1/2}$ and $z = vt$. Thus, in the eikonal approximation the internuclear potential $W(R)$ enters into the theory by providing information about the scattering process through the phase of the scattering amplitude. Hence, a comparison of theoretical results with experimentally determined differential cross sections provides a critical test of the theoretical model because both the magnitude and the phase of the scattering amplitudes are probed. Furthermore, from Eq. (2) it is obvious that a more sensitive test of the eikonal phase occurs for small scattering velocities.

Belkic and Salin[25] introduced the Coulomb-Brinkman-Kramers (CBK) approximation to describe the differential cross sections for charge-transfer processes using the Brinkman-Kramers (BK) approximation to calculate the scattering amplitude $A(b)$ and a Coulomb potential $W_c(R) = Z_T Z_P/R$ (Z_T, Z_P are the target and projectile nuclear charges, respectively) to calculate the eikonal phase. Following this work, the static-Brinkman-Kramers (SBK) approximation was proposed by Rogers and McGuire,[13] here a static potential $W_{S2}(R) = Z_T Z_P(\lambda + 1/R)\exp(-2\lambda R)$ (λ is the screening parameter) is used to replace $W_C(R)$ in order to account for the screening of the target nucleus by the electrons. Both CBK and SBK models are unsatisfactory in that the BK approximation does not predict the experimentally accepted value of the total charge-transfer cross section. However, the work reported in Refs. 13 and 25 demonstrated the importance of the internuclear potential in describing the angular distribution of the capture process. Several other theoretical investigations followed this early work. Lin and Soong[16] used the electron-transfer amplitude calculated from the two-state two-center atomic expansion model and applied the eikonal approximation similar to the CBK and SBK methods. The resulting differential cross sections are in good agreement with the experimental data of Bratton *et al.*[10] A moderate dependence on the selection of the Coulombic or static potentials for the calculation of the eikonal phase was obtained for his high velocity result. Belkic and coworkers[14,18] also made a similar study using the CDW approximation. Their results which are in overall agreement with the experimental results reported in Ref. 10 show some structure not evident in the experimental data and tend to underestimate the very small angle (less than 0.22 mrad in the center-of-mass) experimental values. It should be noted that both the TSAE and the CDW approximations predict the experimentally accepted value of the total capture cross sections at 293 keV.

The early studies mentioned above, though successful in describing the experimental results of Bratton *et al.*,[10] suffer from the fact that the internuclear potentials are introduced in an *ad hoc* manner. In principle, the one-electron Hamiltonian used in all of these model studies should be derived from the *known* many-electron Hamiltonian within the independent electron approximation. Recently, this reduction has been reported by Rivarola *et al.*[19] Assuming that the passive electrons remain at their respective initial states throughout the collision, Rivarola *et al.*[19] derived the appropriate internuclear potential in the one-electron model Hamiltonian which is to be used in calculating differential cross sections for charge-transfer processes. In the case of a helium target, this potential takes the form

$$W_{S1}(R) = \frac{Z_P(Z_T-1)}{R} + Z_P\left(\frac{1}{R}+\lambda\right)\exp(-2\lambda R). \quad (3)$$

This potential reduces to $Z_P Z_T/R$ as $R \to 0$ and to $Z_P(Z_T-1)/R$ as $R \to \infty$. The potential $W_{S1}(R)$ is Coulombic at large R, in contrast to the static screening potential $W_{S2}(R)$, where both the active and the passive electrons are assumed to screen the target nucleus.

In a recent publication, Lin and Tunnell[34] have demonstrated that a combination of the single-active-electron approximation with the TSAE method can provide reasonably good theoretical results when the projectile velocity is less than the target electron-orbital velocity if a realistic potential is used. The internuclear potential $W_{S1}(R)$ is consistent with the techniques used in this work.

The sensitivity of the calculated differential cross sections to the internuclear potential is illustrated in the following section where the "theoretical" results obtained with $W_C(R)$ and $W_{S2}(R)$ are shown. It must be emphasized that when these two representations of the internuclear potential were used to calculate the differential cross section at an incident energy of 293 keV for comparison with the experimental results of Bratton *et al.*[10] no significant differences between the two resulting differential cross sections were observed.[16] The results at lower energies reported in the present work clearly show the inappropriateness of the potentials $W_C(R)$ and $W_{S2}(R)$.

RESULTS AND DISCUSSION

The differential cross sections for electron capture in proton-heilum collisions at 25, 30, 50, and 100 keV resulting from the present experimental and theoretical work are presented in Table I. The experimental results, are for electron capture into all bound states. The theoretical results, which are for capture into the ground state, were calculated in the TSAE model using the potential $W_{S1}(R)$ for calculating the eikonal phase.

The value of the total cross section for electron capture in proton-helium collisions σ_{total} at 25, 30, 50, and 100 keV given in Table I has been obtained from the present theoretical work and from the experimental work reported in Ref. 8. The theoretically determined value of σ_{total} is the result of a numerical integration of $(d\sigma/d\Omega)_{\text{theor}}$. The experimentally determined value of σ_{total} was used to normalize the individual data acquisition sets of the present experimental work.

In Fig. 2 the 30-keV results of the present work are shown graphically. Also shown in this figure are the theoretical results obtained using the internuclear potentials $W_C(R)$ and $W_{S2}(R)$. The three theoretical results are obtained as explained in the previous section using Eq. (1) with the values $A(b)$ calculated from the TSAE model and the potentials $W_C(R)$, $W_{S2}(R)$, and $W_{S1}(R)$ for the calculation of the eikonal phase. The value of λ for the calculations presented in this work is $\lambda = 1.6785$. Obviously, the theoretical results obtained using $W_{S1}(R)$ exhibit the best agreement with the experimentally determined differential cross section.

The dominant feature of the experimentally determined differential cross section shown in Fig. 2 is the distinct change in slope observed at 0.8 mrad. This feature is well reproduced by the theoretical results obtained with $W_{S1}(R)$. Bratton *et al.*[10] reported a similar dependence of the differential cross section on the scattering angle for an incident proton energy of 293 keV. At this higher end of the intermediate velocity range, the change in slope is not as pronounced as that shown by the present results in Fig. 2.

While the representation of the internuclear potential by $W_C(R)$ or $W_{S2}(R)$ is not correct, the theoretical results obtained using these potentials have been included in Fig. 2 because they illustrate the virtue of the theoretically more sound potential $W_{S1}(R)$. When $W_C(R)$ is used to calculate the eikonal phase, the theoretical value of the differential cross section is well below the experimentally determined value at the small scattering angles indicating that the deflection by the unscreened nucleus is much too strong. The internuclear potential $W_{S2}(R)$ provides screening of the target nucleus but it also has the character of a short-range potential as evidenced by the diffraction minimum predicted by the calculation using this potential. It should be noted that this minimum bears no relationship to the Jackson-Shiff-[35] or

TABLE I. Experimentally determined differential cross sections $(d\sigma/d\Omega)_{exp}$ for electron capture into all bound states and theoretically determined differential cross sections $(d\sigma/d\Omega)_{theor}$ for electron capture into the ground state by protons from helium atoms for different laboratory energies. Differential cross sections and scattering angles are in center-of-mass units.

	25 keV		30 keV		50 keV		100 keV	
$\theta_{c.m.}$	$(d\sigma/d\Omega)_{exp}$	$(d\sigma/d\Omega)_{theor}$	$(d\sigma/d\Omega)_{exp}$	$(d\sigma/d\Omega)_{theor}$	$(d\sigma/d\Omega)_{exp}$	$(d\sigma/d\Omega)_{theor}$	$(d\sigma/d\Omega)_{exp}$	$(d\sigma/d\Omega)_{theor}$
(mrad)	(cm^2/sr)		(cm^2/sr)		(cm^2/sr)		(cm^2/sr)	
0.0	$(5.4\pm1.7)\times10^{-10}$	2.20×10^{-10}	$(5.5\pm1.0)\times10^{-10}$	2.43×10^{-10}	$(7.8\pm3.1)\times10^{-10}$	2.03×10^{-10}	$(1.2\pm0.5)\times10^{-10}$	1.10×10^{-10}
0.1	$(3.9\pm0.7)\times10^{-10}$	2.06×10^{-10}	$(4.1\pm0.3)\times10^{-10}$	2.24×10^{-10}	$(3.8\pm0.6)\times10^{-10}$	1.85×10^{-10}	$(9.2\pm1.5)\times10^{-11}$	9.36×10^{-11}
0.2	$(3.4\pm0.5)\times10^{-10}$	1.70×10^{-10}	$(2.8\pm0.1)\times10^{-10}$	1.77×10^{-10}	$(2.1\pm0.2)\times10^{-10}$	1.38×10^{-10}	$(6.1\pm2.4)\times10^{-11}$	5.70×10^{-11}
0.3	$(2.3\pm0.3)\times10^{-10}$	1.23×10^{-10}	$(1.8\pm0.1)\times10^{-10}$	1.19×10^{-10}	$(1.3\pm0.3)\times10^{-10}$	8.40×10^{-11}	$(3.1\pm0.3)\times10^{-11}$	2.48×10^{-11}
0.4	$(1.3\pm0.2)\times10^{-10}$	7.74×10^{-11}	$(1.1\pm0.1)\times10^{-10}$	6.85×10^{-11}	$(6.3\pm0.7)\times10^{-11}$	4.12×10^{-11}	$(1.4\pm0.2)\times10^{-11}$	8.12×10^{-12}
0.5	$(5.9\pm1.1)\times10^{-11}$	4.26×10^{-11}	$(6.0\pm1.2)\times10^{-11}$	3.46×10^{-11}	$(2.8\pm0.9)\times10^{-11}$	1.67×10^{-11}	$(6.3\pm1.2)\times10^{-12}$	2.73×10^{-12}
0.6	$(2.9\pm0.9)\times10^{-11}$	2.10×10^{-11}	$(3.3\pm0.7)\times10^{-11}$	1.62×10^{-11}	$(1.1\pm0.4)\times10^{-11}$	6.76×10^{-12}	$(3.2\pm0.6)\times10^{-12}$	1.52×10^{-12}
0.7	$(1.5\pm0.6)\times10^{-11}$	1.02×10^{-11}	$(1.9\pm0.2)\times10^{-11}$	8.12×10^{-12}	$(5.8\pm1.5)\times10^{-12}$	4.15×10^{-12}		1.15×10^{-12}
0.8	$(8.3\pm3.3)\times10^{-12}$	6.08×10^{-12}		5.23×10^{-12}		3.60×10^{-12}	$(1.4\pm0.2)\times10^{-12}$	9.64×10^{-13}
0.9		4.93×10^{-12}	$(6.1\pm0.9)\times10^{-12}$	4.45×10^{-12}	$(2.5\pm0.6)\times10^{-12}$	3.13×10^{-12}		8.66×10^{-13}
1.0	$(6.2\pm2.8)\times10^{-12}$	4.64×10^{-12}		4.31×10^{-12}	$(2.0\pm0.6)\times10^{-12}$	2.58×10^{-12}		7.71×10^{-13}
1.1		4.42×10^{-12}	$(3.8\pm0.3)\times10^{-12}$	4.22×10^{-12}		2.16×10^{-12}		6.10×10^{-13}
1.2		4.12×10^{-12}		3.99×10^{-12}	$(1.9\pm0.5)\times10^{-12}$	1.94×10^{-12}	$(5.3\pm0.5)\times10^{-13}$	4.39×10^{-13}
1.3	$(4.9\pm2.0)\times10^{-12}$	3.80×10^{-12}	$(2.9\pm0.2)\times10^{-12}$	3.58×10^{-12}		1.81×10^{-12}		3.28×10^{-13}
1.5	$(2.6\pm1.2)\times10^{-12}$	3.16×10^{-12}		2.58×10^{-12}		1.36×10^{-12}		2.49×10^{-13}
1.6		2.77×10^{-12}		2.15×10^{-12}	$(9.9\pm0.5)\times10^{-13}$	1.04×10^{-12}		2.06×10^{-13}
1.7	$(1.4\pm0.9)\times10^{-12}$	2.34×10^{-12}	$(1.8\pm0.2)\times10^{-12}$	1.81×10^{-12}		7.60×10^{-13}	$(2.5\pm0.8)\times10^{-13}$	1.53×10^{-13}
2.0	$(5.9\pm3.8)\times10^{-13}$	1.24×10^{-12}		1.06×10^{-12}	$(8.0\pm0.5)\times10^{-13}$	4.64×10^{-13}		9.50×10^{-14}
2.2		8.83×10^{-13}	$(1.0\pm0.2)\times10^{-12}$	7.31×10^{-13}		3.84×10^{-13}		6.66×10^{-14}
2.5	$(2.4\pm0.8)\times10^{-13}$	5.81×10^{-13}						
3.0	$(8.6\pm5.5)\times10^{-14}$							
σ_{total} (cm^2)	2.1×10^{-16}	1.4×10^{-16}	1.9×10^{-16}	1.3×10^{-16}	1.0×10^{-16}	8.3×10^{-17}	3.0×10^{-17}	2.6×10^{-17}

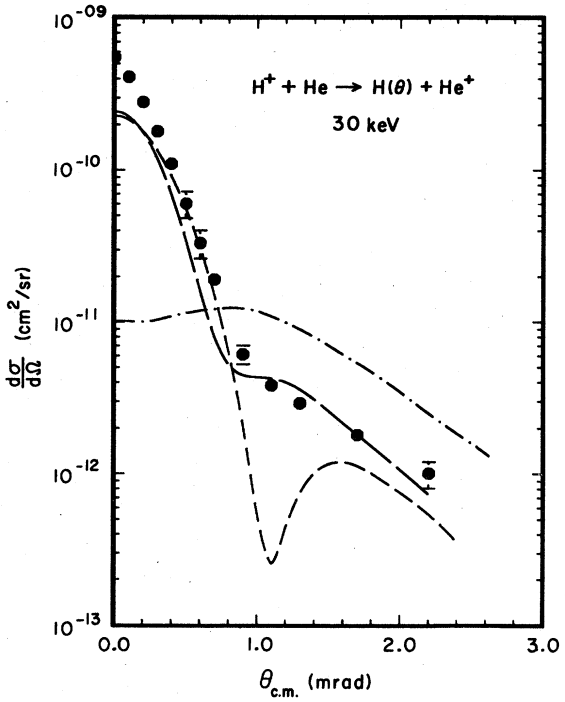

FIG. 2. Differential cross sections for electron capture from helium atoms by protons with a laboratory energy of 30 keV. Closed circles are the present experimental results. The present TSAE theoretical results are for the different internuclear potentials: long dashes, $W_{S1}(R)$; short dashes, $W_{S2}(R)$; dash-dot, $W_C(R)$.

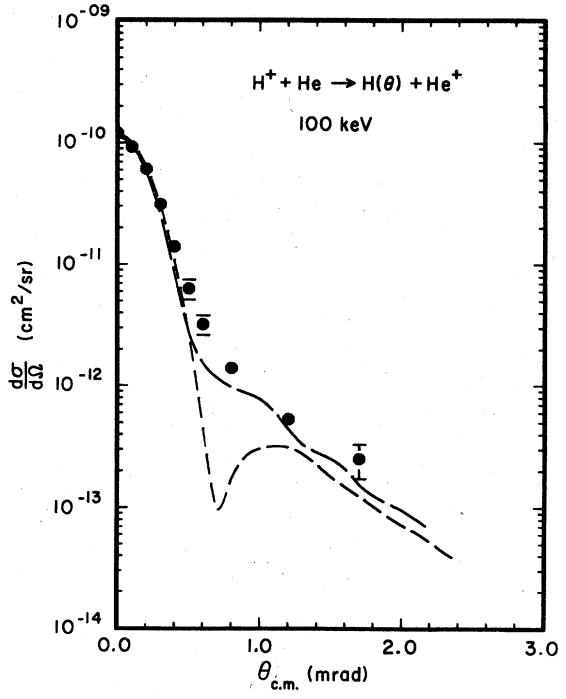

FIG. 3. Differential cross sections for electron capture from helium atoms by protons with a laboratory energy of 100 keV. See Fig. 2 for the legend.

Born (C)-[36] type minima.

Some "discrepancy" between the theoretically and experimentally determined differential cross sections is not unexpected. There is capture into excited states and the angular distribution for higher states need not have the same shape as that of the 1s state. The discrepancy between theory and experiment could also be an indication of the limit of the validity of the two-state two-center atomic expansion method which is not accurate for collisions at small impact parameters.[15,16]

The experimental results at 50 keV are in good agreement with the results of the TSAE calculation when the potential $W_{S1}(R)$ is used. The theoretically determined values of the differential cross section lie below the experimentally determined values at the smaller-scattering angles; as in the case for 30 keV shown in Fig. 2. From a center-of-mass scattering angle of approximately 0.8 mrad on to the 2.0 mrad the agreement between theory and experiment is very good.

In Fig. 3 the experimentally determined differential cross section at an incident energy of 100 keV is compared with the theoretical results of the TSAE calculation using both forms of the "static potential". At this energy the agreement between theory and experiment is extremely good when $W_{S1}(R)$ is used in the calculation.

CONCLUSIONS

The experimentally determined differential cross section for electron capture in collisions of protons with helium atoms reported in this paper are the first experimental results in the 25–100-keV incident proton energy range. The measured differential cross sections for charge exchange include forward scattering in the center-of-mass angles 0–2 mrad. The success of the present investigation demonstrates that the UMR differential ion energy-loss spectrometer can be used to investigate charge-exchange processes. This important additional capability will allow the future investigation of both excitation and charge-exchange processes with the same apparatus.

Both the shape and the magnitude of the differential cross section for electron capture in proton-helium collisions from 25–100 keV is well represented by the eikonal approximation results of the two-state two-center atomic expansion model[15,16] when the representation of the internuclear potential takes into account the effect of the active target electron.[19] The agreement between the theoretically and experimentally determined values of the differential cross section improves with increasing energy.

ACKNOWLEDGMENTS

The experimental work is supported in part by the National Science Foundation. The theoretical work is supported in part by the U. S. Department of Energy, Division of Chemical Sciences. C. D. L. is also partially supported by the Alfred P. Sloan Foundation.

---

*Present address: Physics Department, University of Colorado, Boulder, Colorado 80309.

† Present address: Texas Instruments Incorporated, Semiconductor Research Lab, P.O. Box 225012, Mail Stop 82, Dallas, Texas 72565.

[1]Herbert F. Helbig and Edgar Everhart, Phys. Rev. A 674, 136 (1964).

[2]William Keever and Edgar Everhart, Phys. Rev. A 1, 1083 (1970).

[3]R. H. McKnight and D. H. Jaecks, Phys. Rev. A 4, 2281 (1971).

[4]D. H. Crandall and D. H. Jaecks, Phys. Rev. A 4, 2271 (1971).

[5]R. L. Fitzwilson and E. W. Thomas, Phys. Rev. A 6, 1054 (1972).

[6]E. W. Thomas, *Excitation in Heavy Particle Collisions* (Wiley-Interscience, New York, 1972).

[7]B. M. Doughty, M. L. Boad, and R. W. Cernosek, Phys. Rev. A 18, 29 (1978).

[8]C. F. Barnett, J. A. Ray, E. Ricci, M. I. Wilker, E. W. McDaniel, E. W. Thomas, and H. B. Gilbody, Report No. ORNL-5206, 1977 (unpublished).

[9]A. B. Wittkower and H. B. Gilbody, Proc. R. Soc. London 90, 343 (1967). Only the half-angle of the scattered-atom angular distribution is reported.

[10]T. R. Bratton, C. L. Cocke, and J. R. Macdonald, J. Phys. B 10, L517 (1977).

[11]R. A. Mapleton, *Theory of Charge Exchange* (Wiley-Interscience, New York, 1972).

[12]B. H. Bransden, Rep. Prog. Phys. 35, 949 (1972).

[13]S. R. Rogers and J. H. McGuire, J. Phys. B 10, L497 (1977).

[14]Dz. Belkic and A. Salin, J. Phys. B 11, 3905 (1978).

[15]C. D. Lin, S. C. Soong, and L. N. Tunnell, Phys. Rev. A 17, 1646 (1978).

[16]C. D. Lin and S. C. Soong, Phys. Rev. A 18, 499 (1978).

[17]D. Basu, S. C. Mulherjee, and D. P. Soral, Phys. Rep. 42, 145 (1978).

[18]Dz. Belkic, R. Gayet, and A. Salin, Phys. Rep. 56, 279 (1979).

[19]R. D. Rivarola, R. D. Piacentini, A. Salin, and Dz. Belkic, J. Phys. B 13, 2601 (1980).

[20]R. G. Newton, *Scattering Theory of Waves and Particles* (McGraw-Hill, New York, 1966), p. 582.

[21]J. T. Park, J. M. George, J. L. Peacher, and J. E. Aldag, Phys. Rev. A 18, 48 (1978).

[22]J. T. Park, IEEE Trans. Nucl. Sci. NS-26, 1011 (1979).

[23]J. T. Park, J. E. Aldag, J. L. Peacher, and J. M. George, Phys. Rev. A 21, 751 (1980).

[24]J. E. Aldag, J. L. Peacher, P. J. Martin, V. Sutcliffe, J. George, E. Redd, T. J. Kvale, D. M. Blankenship, and J. T. Park, Phys. Rev. A 23, 1062 (1981).

[25]Dz. Belkic and A. Salin, J. Phys. B 9, L397 (1976).

[26]EMI Gencom Inc. Model 9642/3B.

[27]H. D. Young, *Statistical Treatment of Experimental Data* (McGraw-Hill, New York, 1962), p. 78.

[28]H. Schiff, Can. J. Phys. 32, 393 (1954).

[29]R. J. Glauber, *Lectures in Theoretical Physics, Vol. 1* (Interscience, New York, 1959), p. 315.

[30]J. H. McGuire and L. Weaver, Phys. Rev. A 16, 41 (1977).

[31]R. McCarroll and A. Salin, J. Phys. B 1, 163 (1968).

[32]L. Willets and S. J. Wallace, Phys. Rev. 169, 84 (1968).

[33]J. C. Y. Chen and K. M. Watson, Phys. Rev. 174, 152 (1968).

[34]C. D. Lin and L. N. Tunnell, Phys. Rev. A 22, 76 (1980).

[35]J. D. Jackson and H. Schiff, Phys. Rev. 89, 359 (1953).

[36]K. Omidvar, J. E. Golden, J. H. McGuire, and L. Weaver, Phys. Rev. A 13, 500 (1976).